

## Dynamic Vibration Absorber (DVA) Using Combined Piecewise and Magnetic Stiffness Mechanism

Wan Muhammad Amir<sup>1</sup>, Roszaidi Ramlan<sup>1\*</sup>, Mohd Nazim Abdul Rahman<sup>1</sup>,  
Azma Putra Azis<sup>2</sup>, Abd Rahman Dullah<sup>1</sup> and Kok Swee Leong<sup>3</sup>

<sup>1</sup>Faculty of Mechanical Technology and Engineering, Universiti Teknikal Malaysia Melaka, 76100, Durian Tunggal, Melaka, Malaysia

<sup>2</sup>School of Civil and Mechanical Engineering, Faculty of Science and Engineering, Curtin University, Curtin Perth, Kent Street, Bentley, Western Australia 6102, Australia

<sup>3</sup>Faculty of Electronic and Computer Technology and Engineering, Universiti Teknikal Malaysia Melaka, 76100, Durian Tunggal, Melaka, Malaysia

### ABSTRACT

Linear dynamic vibration absorber (DVA) efficiently suppresses the structural vibration within the 3 dB amplitude frequency bandwidth. Beyond this bandwidth, it may not be effective in suppressing the vibration. In fact, if not properly tuned, it may increase the vibration of the structure. This study examines a DVA mechanism incorporating a unique piecewise and magnetic stiffness combination. By integrating these two types of stiffness, the DVA operates in nonlinear modes, improving its ability to dampen vibrations over a wider frequency range. The positioning of limit blocks and the gap between magnets allows precise control over the level of nonlinearity for each mode, namely, hardening, softening and combined modes. Quasi-static measurements were conducted to analyse the static characteristics of the device for each mode. Dynamic measurements were conducted to analyse the device's dynamic performance in deflection-frequency characteristics, providing insights into the device's response across a frequency range (10 Hz to 50 Hz) for each mode. This evaluation helped assess the proposed mechanism's ability as a DVA to mitigate vibrations with varying frequencies. The measurement results from the three modes were compared. While hardening and softening modes proved to be able to widen the bandwidth, the combined mode was

the most effective one in widening the bandwidth as its operation covers both operating regions of softening and hardening modes. The decrease in the multi-stable solution frequency region ensures that the NDVA operates with a larger amplitude in the vibration suppression region more favourably.

### ARTICLE INFO

#### Article history:

Received: 6 March 2024

Accepted: 21 October 2024

Published: 21 February 2025

DOI: <https://doi.org/10.47836/pjst.33.2.25>

#### E-mail addresses:

[amir9firdaus@gmail.com](mailto:amir9firdaus@gmail.com) (Wan Muhammad Amir)

[roszaidi@utem.edu.my](mailto:roszaidi@utem.edu.my) (Roszaidi Ramlan)

[nazim@utem.edu.my](mailto:nazim@utem.edu.my) (Mohd Nazim Abdul Rahman)

[Azmaputra.Azis@curtin.edu.au](mailto:Azmaputra.Azis@curtin.edu.au) (Azma Putra)

[abdrahman@utem.edu.my](mailto:abdrahman@utem.edu.my) (Abd Rahman Dullah)

[sweeleong@utem.edu.my](mailto:sweeleong@utem.edu.my) (Kok Swee Leong)

\*Corresponding author

**Keywords:** Hardening stiffness, nonlinear dynamic vibration absorber, piecewise stiffness, softening stiffness

## INTRODUCTION

Vibration control is paramount in maintaining the stability of structures and machinery. Passive control strategies, specifically dynamic vibration absorbers (DVAs), have shown remarkable effectiveness in achieving this goal.

The fundamental principle of linear DVAs revolves around designing an absorber with a natural frequency that coincides with the primary structure's resonance frequency, as shown in Figure 1. When these two frequencies match, the vibration of the primary structure will be suppressed, leaving the linear DVA to continue vibrating to counter the motion of the primary structure. The vibration suppression bandwidth of the primary structure  $\Delta\Omega_t$  shown in Figures 2 and 3 depends on the dynamic characteristics of the linear DVA, i.e. the half-power bandwidth of the DVA. However, these linear DVAs face limitations due to their restricted operational bandwidth, which prevents them from effectively functioning when dealing with applications with varying frequencies. The linear DVA must be constantly re-tuned to match the primary structure's resonance frequency to stay effective. Typically, the stiffness will be re-tuned instead of the mass. Constant re-tuning can be made in several ways. They are active (Kassem et al., 2020), adaptive (Guo et al., 2022; Komatsuzaki et al., 2016) and passive tuning (Cheng et al., 2022). Although active and adaptive tuning often results in better performance, the requirement of an external system as part of the tuning mechanism may not be favourable in some applications. On the other hand, passive tuning may perform less but is always chosen due to its simplicity and the absence of an external tuning system.

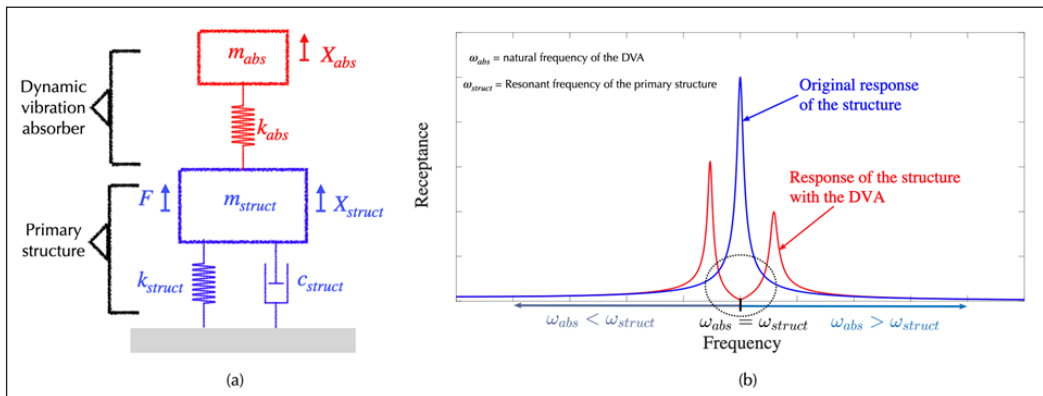


Figure 1. Quasi-static Measurement Setup (a) mass-spring-damper model of the primary structure and the dynamic vibration absorber (DVA), and (b) Frequency of the response function (receptance) of the primary structure with and without the DVA indicating the tuned response ( $\omega_{abs} = \omega_{struct}$ ) and the mistuned response ( $\omega_{abs} < \omega_{struct}$ ,  $\omega_{abs} > \omega_{struct}$ )

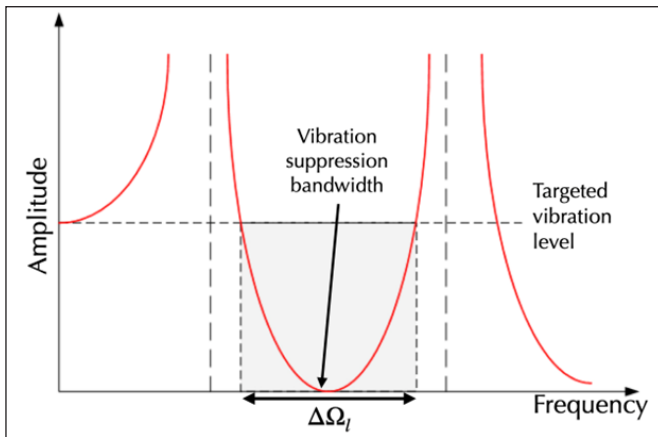


Figure 2. A magnified view of the vibration suppression bandwidth is shown in Figure 1(b) around  $\omega_{abs} = \omega_{struct}$

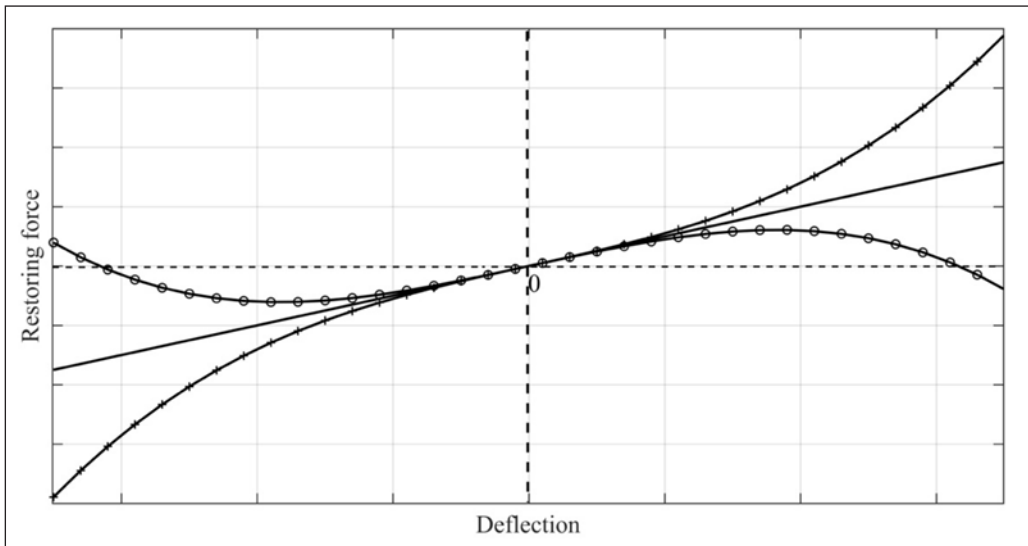


Figure 3. Restoring force versus tip deflection for different modes of stiffness (linear stiffness [solid line], softening stiffness [solid line with circle], hardening stiffness [solid line with plus sign])

The Duffing oscillator transforms the traditional linear system into a nonlinear system, enhancing its capabilities through stiffness adjustments to overcome the need for constant re-tuning (Brennan et al., 2008; Sun & Nagarajaiah, 2019). In the beginning, the primary research on the application of the Duffing oscillator was on vibration-based energy harvesting before embarking on the vibration mitigation application. These two applications benefit from the same system and can be used interchangeably. However, they may be referred to as energy harvesting devices and dynamic vibration absorbers, respectively.

The first aims to harvest energy from the system's motion, and the second is to suppress the vibration of the primary structure as it vibrates. In some applications, both purposes are combined (Kakou et al., 2024).

Numerous researchers have explored nonlinear stiffness mechanisms (Gatti et al., 2019; Li & Cui, 2017; Ramlan et al., 2010), particularly in energy harvesting systems, for their potential to cover a broader frequency spectrum and efficiently capture energy. Usually, two types of nonlinear stiffness mechanisms have been proposed. They are softening (Low et al., 2020; Wang et al., 2020) and hardening (Huang et al., 2021; Sun et al., 2013) stiffness.

The softening system consists of a stiffness which softens as the deflection increases, as shown in Figure 3. It leads to a left-skewed frequency response, as shown in Figure 4. On the other hand, the stiffness of the hardening system hardens with the deflection, thus leading to a right-skewed frequency response. Unlike linear stiffness, the restoring force-deflection characteristics of softening and hardening stiffness no longer satisfy Hooke's law. Hence, DVAs are often termed nonlinear dynamic vibration absorbers (NDVA) when they operate with softening or hardening stiffness. Both the hardening and the softening system frequency responses vary much slower with respect to the frequency compared to the linear system. This slower rate results in the wider half-power bandwidth,  $\Delta\Omega_{NH}$  and  $\Delta\Omega_{NS}$ , respectively.

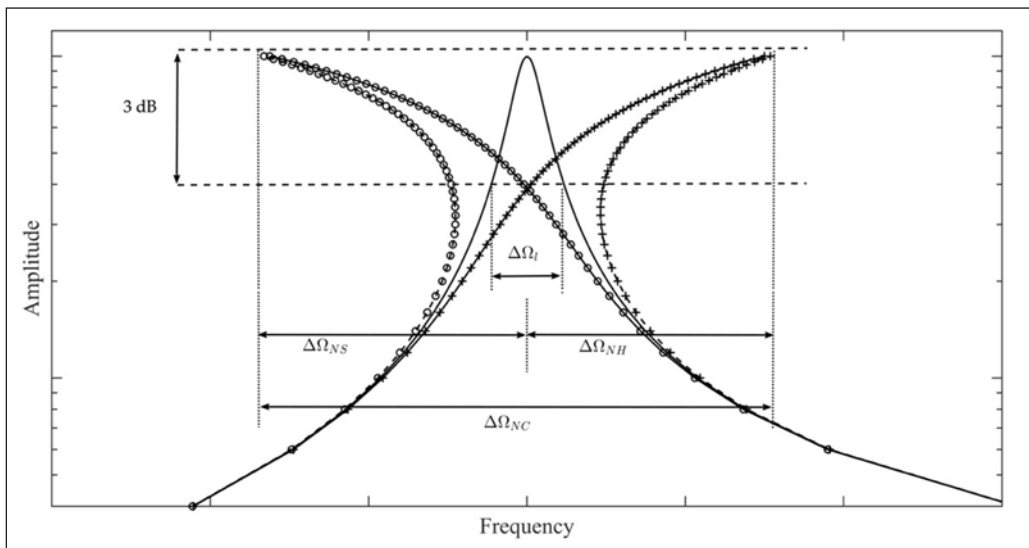


Figure 4. The frequency response function of the respective stiffness modes showing their half-power bandwidth, i.e. linear mode ( $\Delta\Omega_L$ ), hardening mode ( $\Delta\Omega_{NH}$ ), softening mode ( $\Delta\Omega_{NS}$ ) and combined mode [hardening + softening] ( $\Delta\Omega_{NC}$ )

The softening and hardening stiffness can be realised by having magnetic stiffness in attractive and repulsive modes, respectively. The stiffness can be adjusted by altering the

gap between the magnets (Rezaei et al., 2024). In addition, the hardening stiffness can also be realised using a constrained motion (Shui & Wang, 2018; Jin et al., 2022), which is very similar to the piecewise-linear stiffness mechanism. A nonlinear gas-spring hardening mechanism is used to mitigate the vibration of large structures such as buildings (Rong et al., 2023).

Currently, the two nonlinear stiffness mechanisms have been used independently in the application of vibration absorption, i.e. softening (Wang et al., 2020) and hardening (Dou et al., 2023; Jin et al., 2022; Mustaffer et al., 2020). This paper introduces a novel approach to vibration mitigation through a unique DVA design that combines softening and hardening mechanisms in one device. Combining softening and hardening modes in one system aims to widen the effective vibration suppression bandwidth  $\Delta\Omega_{NC}$  even wider than the bandwidth of individual modes. The absorber's ability to operate on hardening and softening stiffness makes it adaptable to various frequency-changing applications, even better than the individual NDVA. Experimental assessments were conducted to evaluate the static and dynamic properties of the absorber and validate its feasibility. However, the study's scope is limited to the absorber's frequency response since the vibration suppression bandwidth depends on the half-power bandwidth of the DVA. Thus, the performance of the absorber is qualitatively determined from the half-power bandwidth of the absorber's response rather than from the suppression bandwidth of the vibrating structure's response.

## METHODS

### Configuration of DVA and Operating Principle

Figure 5 shows the schematic of the proposed NDVA mechanism, which combines softening and hardening mechanisms. The mechanism consists of a cantilevered beam with a tip mass. It will give the linear natural frequency of the NDVA, which is given by

$$\omega_n = \sqrt{\frac{3EI}{mL^3}} \quad [1]$$

where  $E$  is Young's Modulus,  $I$  is the second moment of area,  $m$  is the tip mass, and  $L$  is the length of the beam. A limit block is placed on each side of the beam. The beam hardens as it touches the limit block, resulting in hardening stiffness. The limit block's horizontal  $X$  and vertical  $Y$  distance can be altered. Two stationary and an oscillating magnet produce lateral stiffness, which softens the stiffness of the beam. The stiffness can be altered by varying the gap  $G$ . In this study, individual and combined modes were investigated to justify the benefits of the combined mode.

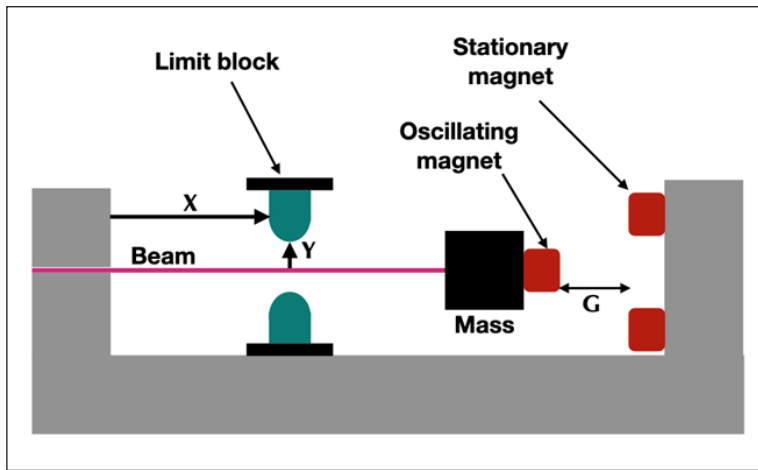


Figure 5. Proposed configurations to generate hardening and softening stiffness by combining the linear stiffness from the beam, piecewise-linear stiffness from the constrained motion and the nonlinear magnetic stiffness

Figure 6 illustrates four distinctive modes of the fabricated dynamic vibration absorber (DVA) system used in the study. At the same time, Table 1 presents the parameters involved in characterising the property of each DVA mode. In particular, Figure 6(a) presents the linear mode configuration, showcasing a cantilever beam paired with a seismic tip mass. The essence of this mode lies in its simplicity, embodying the fundamental principle of DVA operation, i.e. matching its linear natural frequency to the resonance frequency of the structure. For this type of configuration, the length of the beam is usually altered instead of the mass to vary the natural frequency in Equation 1.

Figure 6(b) then delves into the hardening mode, which introduces an intriguing shift in dynamic characteristics. This alteration is achieved by manipulating two tuning parameters, i.e., the horizontal distance  $X$  and the vertical distance  $Y$  of the limit block. These adjustments noticeably influence the system's behaviour, allowing the ability to tune the absorber's response to specific frequency ranges. However, in this study, only the horizontal distance  $X$  was varied, as in Table 1, while the vertical distance  $Y$  was kept constant at 1 mm.

Table 1  
Adjustable parameters for each DVA mode

DVA Mode	Adjustable Parameters (mm)		
	X	Y	G
Linear	-	-	-
	10	1	-
Hardening	20	1	-
	30	1	-
Softening	-	-	1
	-	-	2
	-	-	3
Combined Mode	10	1	1
	20	1	1
	30	1	1

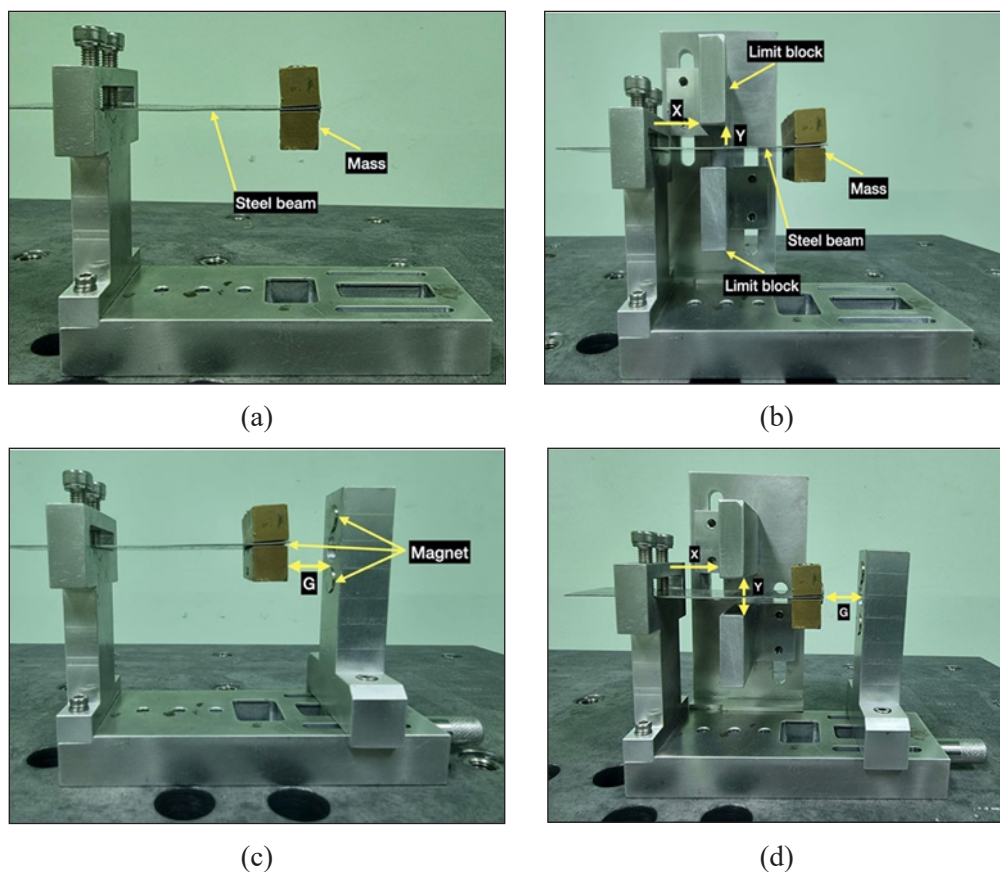


Figure 6. DVA Device in different modes: (a) linear, (b) hardening, (c) softening and (d) combined modes (Dimension of the steel beam: Length = 70 mm, Thickness = 0.1 mm, Width = 26 mm and seismic mass = 48 g)

Moving forward, Figure 6(c) unveils the softening mode, which depends on the gap  $G$  separating repulsive magnets in addition to the existing cantilevered beam and tip mass. Here, the DVA's dynamic characteristics depend on the gap  $G$ . This mode introduces negative stiffness, effectively reducing the overall stiffness.

The culmination of these nonlinear modes is illustrated in Figure 6(d), where a combined configuration is presented. This mode introduces an array of adjustable parameters:  $X$ ,  $Y$  and  $G$  in one device. The combination of these parameters enables the device to either harden or soften the overall stiffness of the system. This adaptive nature allows for tailored responses to applications with varying frequency.

Each DVA mode presented in Figure 6 was characterised statically and dynamically using the adjustable parameters in Table 1. The aim was to investigate the feasibility of the combined mode rather than to compare each mode extensively.

## Quasi-static Measurement

Figure 7 shows the setup for the quasi-static measurements. The NDVA tip mass was excited by the TIRA S51140 electrodynamic shaker at a low frequency, around 1 Hz.

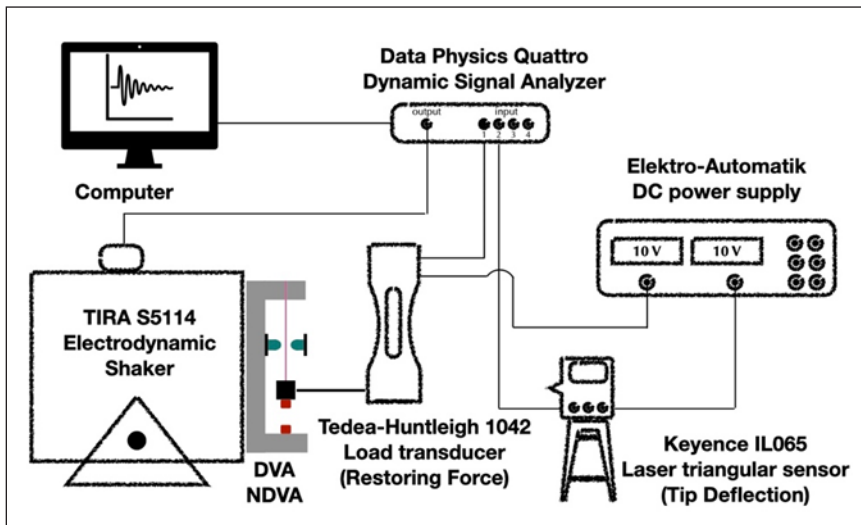


Figure 7. Quasi-static measurement setup

The outcomes of this experiment consist of two key parameters: deflection of the tip mass and restoring force of the beam. A Keyence IL-065 laser triangulation sensor and a Tedeia-huntleigh 1042 load cell were used to measure the deflection of the tip mass and the restoring force of the beam, respectively. The data from the laser sensor and the load cell were recorded using a Data Physics Quattro Dynamic Signal Analyser. These measurements provide an early insight into each configuration's stiffness linearity and nonlinearity.

## Dynamic Measurement

The dynamic measurement setup is shown in Figure 8. The NDVA was placed and excited on an ETS L215M electrodynamic shaker. The Vibration Research Medallion II shaker controller was utilised to maintain the excitation level. During measurement, the absorber was subjected to harmonic excitation within a frequency range from 10 to 50 Hz. The nonlinearity requires the device to be excited in an ascending frequency sweep (10 to 50 Hz) and a descending frequency sweep (50 to 10 Hz) with identical frequency increments. The input displacement was maintained at 1 mm (pk-pk) at a sweep rate of 30 Hz/s, controlled by the feedback signal from the input accelerometer.

The acceleration of the tip mass that represents the output and the input acceleration were measured using Dytran 3225F1 accelerometers. Subsequently, the results from the

measurements were used to construct the frequency response curve in the form of the deflection of the tip mass against the excitation frequency. The sweep-up and sweep-down responses are plotted together in one graph. The deflection-frequency response curves provide a comprehensive understanding of the characteristics of each configuration across frequencies. This exploration allows for insightful observations regarding how the DVA's dynamic characteristics evolve in response to changing parameters, shedding light on the efficacy and adaptability of the proposed design.

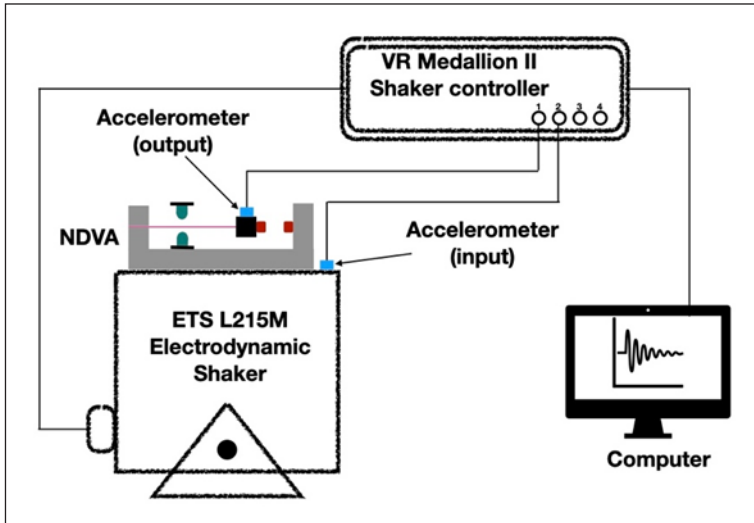
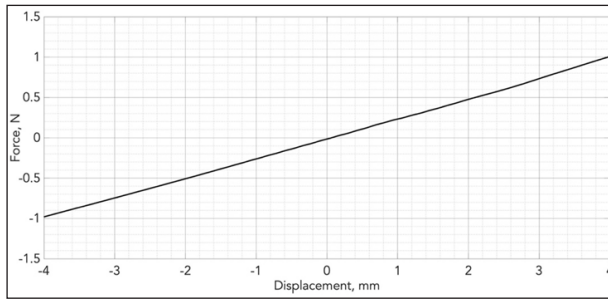


Figure 8. Dynamic measurement setup

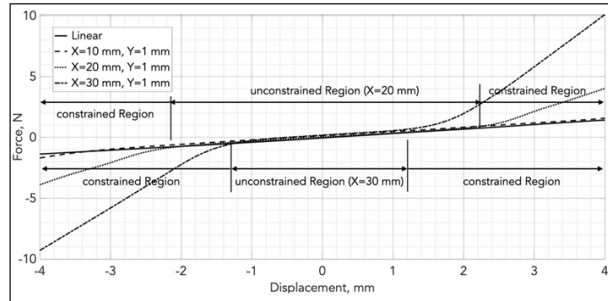
## RESULTS AND DISCUSSIONS

Figure 9 presents comprehensive quasi-static behaviours exhibited by the device across different modes of operation. In the linear mode, as shown in Figure 9 (a), the force-deflection graph highlights a direct and linear correlation between the restoring force of the beam and the deflection of the tip mass. This linear relationship signifies that as the restoring force of the beam increases, the deflection follows proportionately, resulting in a constant stiffness. However, this holds only when the beam remains within its elastic deformation range, governed by the principles of Hooke's law.

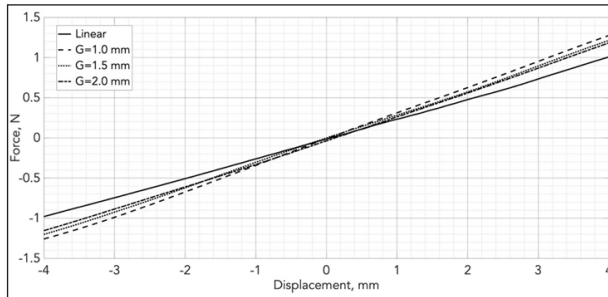
Moving to Figure 9 (b), the force-deflection graph from the hardening mode shows different force-deflection characteristics in two distinct regions, i.e., constrained and unconstrained. The unconstrained region depicts a linear behaviour similar to the linear configuration in Figure 9(a), where the deflection and force relationship remains proportionate. In this region, the motion of the beam was not constrained by the limit blocks. On the other hand, the constrained region reveals a departure from linearity due to



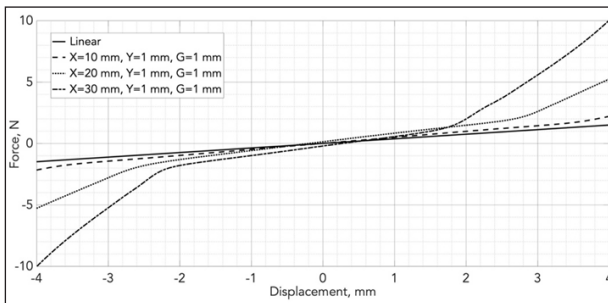
(a)



(b)



(c)



(d)

Figure 9. The quasi-static response of the DVA for (a) linear, (b) hardening, (c) softening, and (d) combined modes

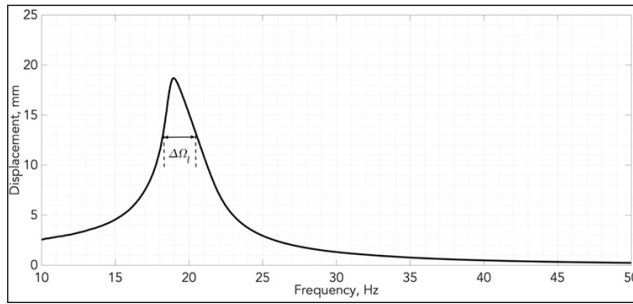
the restricted motion of the beam by the limit blocks, as shown in Figure 6(b). This motion restriction triggers a shift into nonlinear characteristics. Notably, the constrained region increases with the horizontal distance  $X$ , inducing a larger degree of hardening nonlinearity.

Figure 9 (c) shows the quasi-static measurement results for the softening mode. In this mode, the overall stiffness comprises the stiffness from the beam and the magnetic stiffness from the repulsive magnets. Interestingly, altering the distance between the magnets impacts the overall linear stiffness (around the equilibrium position) and the nonlinear stiffness (around the maximum deflection). A decrease in gap  $G$  increases the linear stiffness and softens the nonlinear stiffness. The behaviour might not be visible in the quasi-static measurement yet but will be visible in the dynamic measurement in the later discussion.

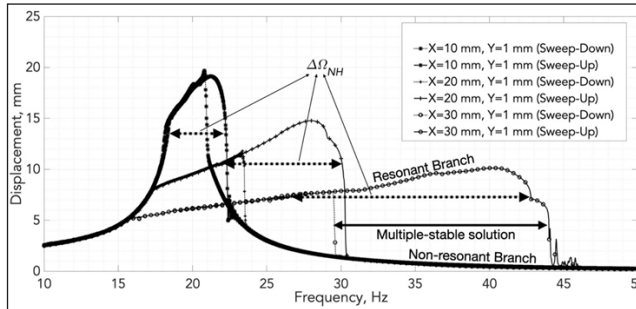
Figure 9 (d) combines these modes, i.e. hardening and softening, into one device. In this case, the force-deflection graph captures the combined effects of the two modes. In the constrained region, the hardening mode prevails, reflecting nonlinearity due to the motion restriction by the limit blocks. Conversely, in the unconstrained region, the magnetic stiffness dictates the linear stiffness around the equilibrium position. The linear stiffness is no longer constant in the unconstrained region, i.e. as a hardening mode in Figure 9(b), due to the influence of the magnetic stiffness.

Figure 10 portrays the dynamic responses of different DVA modes under sweep-up and sweep-down harmonic excitation. The linear mode in Figure 10(a) produces a similar response in sweep-up and sweep-down excitations due to the monotonic nature of the linear response. The adequate frequency bandwidth of the linear mode DVA in suppressing the vibration is closely related to its half-power bandwidth frequency, as denoted by  $\Delta\omega$ . The inclusion of the limit blocks hardens the overall stiffness of the system, as indicated by the right skewness of the dynamic response in Figure 10(b). The frequency sweep-up response follows the resonant branch (larger amplitude). In comparison, the frequency sweep-down response (smaller amplitude) follows the non-resonant branch—the slow rate of amplitude change against the frequency on the resonant branch results in a wider bandwidth. The bandwidth is related to the size of the constrained region shown in Figure 9(b), i.e. the larger the constrained region, the larger the bandwidth. Increasing the horizontal distance  $X$  can realise a large, constrained region. However, the nonlinearity induces a multi-stable solution region in which the response can either be on the resonant or non-resonant branches. The initial conditions solely determine the type of response in this region. The response must be on the resonant branch for the DVA application to provide a large counterforce to the vibrating structure for a wide frequency range. Operating on the non-resonant branch is less effective for a DVA application. In practice, however, the bandwidth can be less than the one presented in Figure 10(b) due to the interchanging response between the two branches.

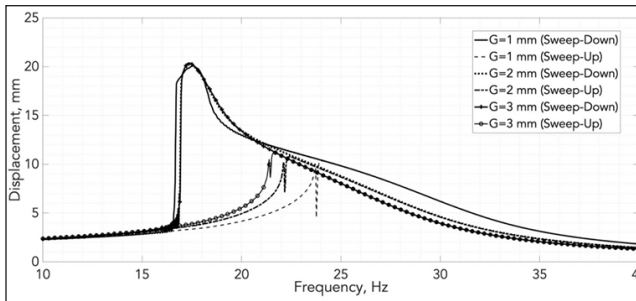
The inclusion of double repulsive magnets, on the other hand, softens the stiffness, which skews the dynamic response to the left, as shown in Figure 10(c). The half-power



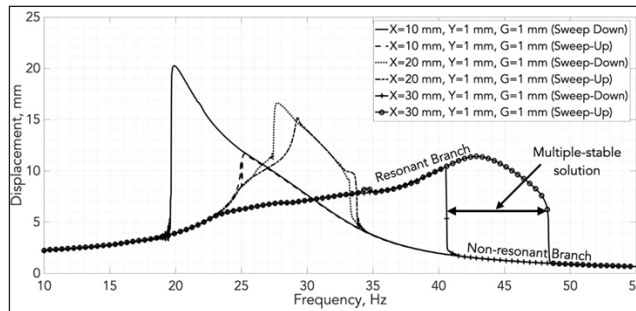
(a)



(b)



(c)



(d)

Figure 10. The dynamic response of the DVA for (a) linear, (b) hardening, (c) softening, and (d) combined modes

bandwidth is still greater than the linear mode but less than the hardening mode. Similar to the hardening mode, the response of the softening mode is also made up of two branches, i.e. resonant and non-resonant. As in the previous mode, the existence of these branches results in the multi-stable solution regions. Based on Figure 10(c), the multi-stable solution region increases with the decrease in the gap  $G$ .

Figure 10(d) shows the dynamic response of the combined mode, which combines hardening and softening modes in one device. The response of the combined mode can be tuned accordingly by adjusting  $X$ ,  $Y$  and  $G$ . Due to the combined adjustable parameters, the response may behave similarly to softening or hardening modes. As discussed in the quasi-static results, the magnetic stiffness dictates the response characteristics considering the same  $X$  and  $Y$  parameters as in the hardening mode. The softening magnetic stiffness overpowers the hardening stiffness due to the restricted motion for small, constrained regions, i.e. small  $X$ , resulting in a softening-like response.

On the other hand, as the constrained region gets larger, i.e. large  $X$ , the hardening stiffness dictates the response, producing a hardening-like response. During the dynamic characterisation with  $X$  set at 20 mm,  $Y$  at 1 mm, and  $G$  at 1 mm, the sweep-up and sweep-down processes produced nearly identical patterns. It suggests that the system can exhibit a near-linear behaviour in both sweep directions at specific positions. The combined mode might be more beneficial as a DVA due to the smaller multi-stable solution region when both modes are positioned at the same distance from the limit blocks, specifically  $X$  at 30 mm, focusing on the hardening-like response. The smaller multi-stable solution region ensures that the response is on the resonant branch, thus enhancing its ability to suppress the vibration effectively. In addition, a variety of dynamic characteristics of the DVA can be altered to suit the target vibration to be suppressed.

## CONCLUSION

Existing hardening and softening mechanisms prove their ability to widen the half-power bandwidth better than the traditional linear mechanism by skewing the frequency response of the DVA to the right or left, respectively. The study presented here shows that integrating hardening and softening stiffness into the design results in a remarkable expansion of the operational bandwidth of dynamic vibration absorbers (DVAs). By adjusting the tuning parameters  $X$ ,  $Y$  and  $G$ , the effective frequency region of the DVA can be altered using only one device instead of two individual nonlinear mode DVAs. Its bandwidth-widening ability and ease of tunability may benefit vibration mitigation in broadband excitation applications such as pipe vibration due to flow turbulence and variation in the input flow rate. The combined mode DVA also shows a reduction in the multi-stable solution region, which addresses possible drawbacks of the hardening mode DVA. A smaller multi-stable solution region minimises the likelihood of the response engaging with the non-resonant

branch, thereby enhancing the effectiveness and reliability of the system. Although the combined mode outperforms the individual modes, its performance depends on the actual suppression bandwidth, which may require independent tuning of  $X$ ,  $Y$  and  $G$ .

While the hardening mode using piecewise-linear stiffness responds well to the alteration of tuning parameters, the sensitivity of the tuning mechanism of the softening mode can be improved. It can be done by either using stronger magnets or adjusting the vertical distance of the stationary magnets. The scope of investigating the performance of the NDVA to mitigate the vibration of the primary structure shall not be limited to harmonic excitation and shall be expanded to random excitation.

## ACKNOWLEDGEMENT

The project is funded by the Ministry of Higher Education Malaysia through the Fundamental Research Grant Scheme (FRGS), No. FRGS/1/2020/FKM-CARE/ F00433. The authors would also like to acknowledge the support from Universiti Teknikal Malaysia Melaka (UTeM)

## REFERENCES

- Brennan, M. J., Kovacic, I., Carrella, A., & Waters, T. P. (2008). On the jump-up and jump-down frequencies of the Duffing oscillator. *Journal of Sound and Vibration*, 318(4–5), 1250–1261. <https://doi.org/10.1016/J.JSV.2008.04.032>
- Cheng, Y., Peng, Z., Wen, H., Song, H., & Cui, Z. (2022). Design of multi-mode low-frequency vibration suppressor based on dynamic vibration absorption principle. *International Journal of Acoustics and Vibration*. 27(3), 265-275. <https://doi.org/10.20855/ijav.2022.27.31870>
- Dou, J., Yao, H., Cao, Y., & Wang, Z. (2023). Permanent magnet based nonlinear energy sink for torsional vibration suppression of rotor systems. *International Journal of Non-Linear Mechanics*, 149, Article 104321. <https://doi.org/10.1016/j.ijnonlinmec.2022.104321>.
- Gatti, G., Brennan, M. J., & Tang, B. (2019). Some diverse examples of exploiting the beneficial effects of geometric stiffness nonlinearity. *Mechanical Systems and Signal Processing*, 125, 4–20. <https://doi.org/10.1016/J.YMSSP.2018.08.024>
- Guo, X., Zhu, Y., Qu, Y., & Cao, D. (2022). Design and experiment of an adaptive dynamic vibration absorber with smart leaf springs. *Applied Mathematics and Mechanics*, 43(10), 1485-1502. <https://doi.org/10.1007/s10483-022-2905-6>
- Huang, H., Yuan, Z., & Liu, W. (2021). Design strategy for optimising the bandwidth of the hardening vibration generator with customised response. *Sensors and Actuators A: Physical*, 332, Article 113197. <https://doi.org/10.1016/J.SNA.2021.113197>
- Jin, Y., Liu, K., Xiong, L., & Tang, L. (2022). A non-traditional variant nonlinear energy sink for vibration suppression and energy harvesting. *Mechanical Systems and Signal Processing*. 181, Article 109479. <https://doi.org/10.1016/j.ymssp.2022.109479>.

- Kakou, P., Gupta, S. K., & Barry, O. (2024). A nonlinear analysis of a *Duffing oscillator* with a nonlinear electromagnetic vibration absorber–inserter for concurrent vibration mitigation and energy harvesting. *Nonlinear Dynamics*, *112*(8), 5847–5862. <https://doi.org/10.1007/s11071-023-09163-6>
- Kassem, M., Yang, Z., Gu, Y., Wang, W., & Safwat, E. (2020). Active dynamic vibration absorber for flutter suppression. *Journal of Sound and Vibration*, *469*, Article 115110. <https://doi.org/10.1016/j.jsv.2019.115110>
- Komatsuzaki, T., Inoue, T., & Terashima, O. (2016). Broadband vibration control of a structure by using a magnetorheological elastomer-based tuned dynamic absorber. *Mechatronics*, *40*, 128–136. <https://doi.org/10.1016/j.mechatronics.2016.09.006>
- Li, L., & Cui, P. (2017). Novel design approach of a nonlinear tuned mass damper with duffing stiffness. *Journal of Engineering Mechanics*, *143*(4), Article 04017004. [https://doi.org/10.1061/\(asce\)em.1943-7889.0001229](https://doi.org/10.1061/(asce)em.1943-7889.0001229)
- Low, P., Ramlan, R., Ghani, H. A., & Muhammad, N. S. (2020). Experimental analysis on the transduction coefficient of a nonlinear electromagnetic energy harvesting device with softening stiffness. *International Journal of Automotive and Mechanical Engineering*, *7*(2), 7816–7831. <https://doi.org/10.15282/ijame.17.2.2020.01.0582>
- Mustaffer, M. H., Ramlan, R., Nazim, M., Rahman, A., & Putra, A. (2020). Experimental characterisation and performance of dynamic vibration absorber with tunable piecewise-linear stiffness. *Journal of the Brazilian Society of Mechanical Sciences and Engineering*, *42*(3), Article 355. <https://doi.org/10.1007/s40430-020-02435-x>
- Ramlan, R., Brennan, M. J., Mace, B. R., & Kovacic, I. (2010). Potential benefits of a nonlinear stiffness in an energy harvesting device. *Nonlinear Dynamics*, *59*(4), 545–558. <https://doi.org/10.1007/s11071-009-9561-5>
- Rezaei, M., Talebitooti, R., Liao, W. H., & Friswell, M. I. (2024). A comparative study on vibration suppression and energy harvesting via mono-, bi-, and tri-stable piezoelectric nonlinear energy sinks. *Nonlinear Dynamics*, *112*(13), 10871–10910. <https://doi.org/10.1007/s11071-024-09562-3>
- Rong, K., Lu, Z., Zhang, J., Zhou, M., & Huang, W. (2023). Nonlinear gas-spring DVA for seismic response control: Experiment and numerical simulation, *Engineering Structures*, *283*, Article 115940. <https://doi.org/10.1016/j.engstruct.2023.115940>.
- Shui, X., & Wang, S. (2018). Investigation on a mechanical vibration absorber with tunable piecewise-linear stiffness. *Mechanical Systems and Signal Processing*, *100*, 330–343. <https://doi.org/10.1016/J.YMSSP.2017.05.046>
- Sun, C., Eason, R. P., Nagarajaiah, S., & Dick, A. J. (2013). Hardening *Düffing oscillator* attenuation using a nonlinear TMD, a semi-active TMD and multiple TMD. *Journal of Sound and Vibration*, *332*(4), 674–686. <https://doi.org/10.1016/j.jsv.2012.10.016>
- Sun, C., & Nagarajaiah, S. (2019). Study of a novel adaptive passive stiffness device and its application for seismic protection. *Journal of Sound and Vibration*, *443*, 559–575. <https://doi.org/10.1016/j.jsv.2018.12.015>

Wang, X., Wu, H., & Yang, B. (2020). Nonlinear multi-modal energy harvester and vibration absorber using magnetic softening spring. *Journal of Sound and Vibration*, 476, Article 115332. <https://doi.org/10.1016/j.jsv.2020.115332>